A NUMERICAL STUDY OF COSSERAT BEAM THEORY APPLIED TO THE MODELING SLENDER STRUCTURES

Adailton Silva Borges[1], adailton@utfpr.edu.br
Adriano Silva Borges[1], adrianoborges@utfpr.edu.br
Albert Willian Faria[2] , albertfaria@unifei.edu.br
Domingos Alves Rade [3], domingos@ufu.br
Aristeu da Silveira Neto [3], aristeus@ufu.br

[1] Federal Technologic University of Paraná – School of Mechanical Engineering, Campus Cornélio Procópio, 86300-000, Cornélio Procopio – PR, Brazil.
[2] Federal University of Itajubá - School of Engineering, Campus of Ibatira, 35900-373, Itabira - MG, Brazil.
[3] Federal University of Uberlândia - School of Mechanical Engineering, Campus Santa Mônica, 38400-902, Uberlândia - MG, Brazil.

Abstract. This work is dedicated to present the development, implementation and assessment of a procedure for modeling tridimensional slender structures, like beams, bars, cables, and more specifically undersea risers, based on nolinear Cosserat beam theory. This approach has the advantage of taking into account geometric nonlinearities, usually neglected by traditional methods. In order to analyze the dynamic behavior of the structure, the deformed configuration of the beam is described by the displacement vector of the curve of centroids, and by a moving vector basis, rigidly attached to the beam cross section, related to an inertial reference frame. The main advantage of this approach is that it is geometrically exact. After that, the discretization of the equations of motion for the structure is performed using the Finite Element Method. To perform the static validation, the results obtained using the algorithm based on Cosserat Theory and the results simulated using the ANSYS® software were compared with experimental data. In order to carry out the dynamic validation, the test structure was analyzed using the implemented algorithm and the results obtained were confronted with results from literature. After the validation, several tests were performed to identify a sufficiently robust integration method to solve the nonlinear equations inherent to the used approach. Finally, using a test structure, it was possible to compare the results from the Cosserat beam theory with those obtained using the Euler-Bernoulli classic theory.

Keywords: Cosserat beam theory, structural dynamics, slender structures, finite elements.

1. INTRODUCTION

In the context of off-shore industry, flexible risers are shallow structural components designed with the purpose of transporting the pressured oil from the well to the platform. Their design involves technological challenges as they are becoming increasingly longer as a result of deeper oil exploitation. Also, during their operation they are subjected to very complex scenarios, resulting from the combination of static and dynamic loads such as: internal pressure, self-weight, residual stress resulting from the installation procedure and vibrations induced by water motion (vortex-induced vibrations-VIV) and the vertical motion of the platform. Thus, the safe and cost-effective design of such structures requires a deep understanding of their mechanical behavior, which can be improved by the use of numerical models capable of accounting for the actual geometry and load conditions, especially fluid-structure interaction.

Pesce (1997) discusses the behavior of long risers, stating that they can be better represented by the theory of flexible lines than the classical beam theory, due to their slender profile. In this context, the author refers to the Cosserat beam theory. This nonlinear theory was developed in the XVIIth century by the Cosserat brothers, and has been revisited and applied to engineering problems in the last few years, as the increase of computer power enables dealing with highly nonlinear differential equations.

As opposed to traditional Euler-Bernoulli or Timoshenko beam theories, the Cosserat beam theory is geometrically exact, in the sense that it is not based on geometric approximations. In this theory, the deformed configuration of the beam is described by the displacement vector of the centroid curve and an orthonormal moving frame, rigidly attached to the cross section of the beam. The orientation of the orthonormal moving frame with respect to an inertial system is parameterized using three consecutive elementary rotations. Thus, the equations of motion are nonlinear differential equations in terms of time and space variables. For static problems, the equilibrium equations become nonlinear ordinary differential equations in terms of a space variable, which can be approximately solved by using standard techniques such as the perturbation approach.

Aiming at solving the nonlinear equations of motion, Simo (1985) and Vu-Quoc et al. (1986) combined the finite element theory to the formulation. In this condition, the displacement functions of the beam are obtained as a function of the nodal displacements and rotations. The main advantage of this procedure is related to the fact that the shape functions are obtained from differential equations of motion, and therefore take into account all the nonlinearities of the system. Consequently, one can ensure satisfactory accuracy of response predictions by dividing the structure in a

number of elements which is significantly smaller than the number required by finite element discretization, based on low order polynomial shape functions.

Recent publications like Alamo (2006) used that methodology, from the second order shape function, to model slender structures, with applications in oil drilling columns. Also, Santos (2005) applied the methodology, but instead used as shape functionslow order polynomial for modeling submerged cables from an initial configuration of equilibrium and excited by the motion of the platform and by the flow of sea water obtained empirically using the Morison's equations.

In the context presented above, one of the objectives of the present work is to define an integration method sufficiently robust, as well the assessment of the order of approximations of the shape functions. Thus, several numerical simulations were performed to evaluate different integration methods and the order of approximations of the shape functions (second and third order). The simulations consisted of a test structure subjected to a force, which was applied in the form of a step function. In order to verify the convergence of the integration methods when the structure is subjected to different degrees of nonlinearity due the increasing of the transversal displacement of the structure, the amplitude of the force was gradually increased for each simulated case.

2. MATHEMATIC MODEL FOR STRUCTURE

One of the most important features of this theory is how the beam is spatially defined in terms of motion of the line passing through their cross sections centroids, defined by the vector $\mathbf{r}(s,t)$ in a Cartesian fixed (inertial) base represented by $F=\{\mathbf{e}_1,\mathbf{e}_2,\mathbf{e}_3\}$ with unit vectors $\mathbf{e}_i$, and a set of orthogonal unit vectors attached to the cross section, forming the basis $S=\{\mathbf{d}_1(s,t),\mathbf{d}_2(s,t),\mathbf{d}_3(s,t)\}$, where the variable s represents the position of the cross section along the line of centroids. Therefore, for each point on the curve formed by the centroids there is an orthonormal moving frame, formed by the unit vector $\mathbf{d}_i(s,t)$, that are defined externally to the position vector $\mathbf{r}(s,t)$. Figure1 shows a schematic representation of a segment of Cosserat beam, which is represented in the two bases mentioned previously.

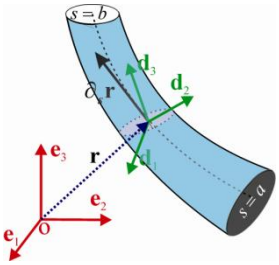

Figure 1 - Schematic model of an element of Cosserat.

For convenience, it is assumed that $\mathbf{d}_1(s,t)$ and $\mathbf{d}_2(s,t)$ are contained in the plane of cross section and, as a consequence, $\mathbf{d}_3(s,t)$ is perpendicular to that plane.

According to the Cosserat beam theory, the strains are classified in two groups: linear strain $\mathbf{v}(s)$ and angular strain $\mathbf{u}(s)$. The components $\mathbf{v}_1(s)$ and $\mathbf{v}_2(s)$ are called shear strain and $\mathbf{v}_3(s)$ is named elongation, while $\mathbf{u}_1(s)$ and $\mathbf{u}_2(s)$ are described as bending strain, $\mathbf{u}_3(s)$ is called the torsion strain.

The relationship between linear and angular deformation, to which a segment of Cosserat beam is subjected, and the fixed and moving bases are established to provide a complete description, that is, the spatial position of the centroids as well as the rotation of the cross-section. Thus, the vector of linear deformation is given in terms of torsion angles and rotation of the cross section, and these relations are used later in the dynamic analysis. In this work these analytical developments were intentionally omitted, but the mathematical details can be found in Cao et al. (2006) and Borges (2010).

2.1 THE GOVERNING EQUATIONS OF MOTION

The local dynamic behavior of a differential element of Cosserat beam with density $\rho(s)$ and cross section area $A(s)$, as obtained by Antman (1995), is given by the following partial differential equations:

$$\frac{\partial \mathbf{h}(s,t)}{\partial t} = \frac{\partial \mathbf{m}(s,t)}{\partial s} + \mathbf{v}(s,t)\times\mathbf{n}(s,t) + \mathbf{l}(s,t) \tag{1}$$

$$\rho(s)A(s)\frac{\partial^2\mathbf{r}(s,t)}{\partial t^2}=\frac{\partial\mathbf{n}(s,t)}{\partial s}+\mathbf{f}(s,t) \tag{2}$$

It can be observed that Eqs.(1)-(2) result from the application of the Newton-Euler principles to the differential beam element. In such equations, $\mathbf{n}(s,t)$, $\mathbf{m}(s,t)$, $\mathbf{h}(s,t)$, $\mathbf{f}(s,t)$ e $\mathbf{l}(s,t)$ are, respectively, the contact force, the contact torque, the angular momentum, the external force and the external torque, all defined per unit of length.

One of the main problems associated to the finite element method is the choice of the shape functions. These functions are responsible for determining the displacement field inside the element from the nodal displacements. In the classic methods, they are usually approximated using low order polynomials. In contrast, in the Cosserat beam theory, the shape functions can be obtained from the differential equations of static equilibrium; hence, they can take into account the system nonlinearities. Consequently, the accuracy of the dynamic response can be improved by dividing the structure in few elements, the number of which is usually much lower than the number required by the traditional beam finite elements.

In the Cosserat beam theory, the displacements,given as a function of nodal displacements and rotations, are obtained from the resolution of the equations of static equilibrium. Nevertheless, for the static equilibrium, the equations of motion become ordinary differential equations, where *s* is the only independent variable. In the literature, the static equilibrium is understood as the absence of external forces, and from Eq.(1), the contact forces must satisfy the condition:

$$\frac{d\mathbf{n}(s)}{ds}=0 \tag{3}$$

and, from Eq.(2), the contact torque density satisfies:

$$\frac{d\mathbf{m}(s)}{ds}+\mathbf{v}(s)\times\mathbf{n}(s)=0 \tag{4}$$

Once defined the main vectors quantities involved in Eqs.(3)-(4), as described by Borges (2010), it is necessary to obtain $\mathbf{m}(s)$ and $\mathbf{n}(s)$ in terms of deformations $\mathbf{u}(s)$ and $\mathbf{v}(s)$. These can be obtained from the constitutive relations of the material. It must be pointed out that, in this work, it was used a constitutive model where the characteristics of a linear elastic material were adopted, based on the constitutive relations of Kirchhoff (Caoet al., 2005). Thus, it is assumed that the Young modulus *E*, the shear modulus *G* and the specific mass along the Cosserat beam element are only function of the spatial variable *s* , and the center of mass coincides with the centroid of the cross-section.

Therefore, using these relations, the forces and torque of contact are given as functions of linear and angular deformations, respectively (Borges, 2010) and, as a result, Eqs.(3)-(4) can be written in terms of the forces and contact moments in the form of a highly nonlinear system, given by:

$$n_1'(s)=u_3(s)n_2(s)-u_2(s)n_3(s) \tag{5}$$

$$n_2'(s)=u_1(s)n_3(s)-u_3(s)n_1(s) \tag{6}$$

$$n_3'(s)=u_2(s)n_1(s)-u_1(s)n_2(s) \tag{7}$$

$$m_3'(s)=u_2(s)m_1(s)-u_1(s)m_2(s) \tag{8}$$

In order to determine the shape functions, it is necessary to solve the nonlinear system given by Eq.(5)-(8). It can be noted that those equations cannot be solved by direct integration. Therefore, the perturbation method will be used in order to obtain an approximated solution. For this purpose, it was used a perturbation method oriented to this nature of solution and, among several available methods, it was chosen the method of Frobenius (Arfken et al., 2000).

According to the Frobenius's method, the following approximations for the shape functions can be found:

$$x(s)=\bar{x}(\bar{s})L=\varepsilon x_1(s)+\varepsilon^2 x_2(s)+\varepsilon^3 x_3(s) \tag{9}$$

$$y(s) = \bar{y}(\bar{s})L = \varepsilon y_1(s) + \varepsilon^2 y_2(s) + \varepsilon^3 y_3(s) \tag{10}$$

$$z(s) = \bar{z}(\bar{s})L = s + \varepsilon z_1(s) + \varepsilon^2 z_2(s) + \varepsilon^3 z_3(s) \tag{11}$$

$$\varphi(s) = \bar{\varphi}(\bar{s})L = \varepsilon \varphi_1(s) + \varepsilon^2 \varphi_2(s) + \varepsilon^3 \varphi_3(s) \tag{12}$$

It must be emphasized that these functions can be approximated to the order required by the user, but the computational costs are drastically increased for higher orders. At first in this work, it was adopted an approximation of second order. At last, approximations of third order were used when it was observed an astonishing number of terms present in these functions. However, the algorithm presented better accuracy for the representation of systems subjected to large displacements.

It is important to emphasize that these displacement functions obtained from static equilibrium will later be used in the dynamic analysis, which eliminates one of the main problems usually found in the classic finite element theory, which is to define conveniently the shape functions.

By associating the shape functions with the extended Hamilton principle it is possible to find the Lagrange equations, which constitute a very convenient way to obtain the equations of motion of dynamical systems. The global equations of motion, given in Eq. (3), are assembled similarly to the classic theory of finite elements. The equations presented below were obtained using symbolic manipulation software. Due to the complexity of their individual terms, they were intentionally omitted here. A more detailed description about this implementation and the construction of the global matrices of the system can be found in Cao et al. (2005) and Borges (2010).

$$\mathbf{M}^{(e)}\ddot{\mathbf{q}}^{(e)}(t) + \mathbf{K}^{(e)}\mathbf{q}^{(e)}(t) + \mathbf{g}^{(e)}\left(\mathbf{q}^{(e)}(t)\right) = \mathbf{f}^{i(e)}(t) + \mathbf{f}^{c(e)}(t) + \mathbf{f}^{d(e)}\left(t, \mathbf{q}^{(e)}\right), \tag{13}$$

where $\mathbf{M}^{(e)}$ is the mass matrix, $\mathbf{K}^{(e)}$ is the linear stiffness matrix, $\mathbf{g}^{(e)}(\mathbf{q}^{(e)}(t))$ is a nonlinear vector with quadratic and cubic terms on the components of $\mathbf{q}^{(e)}$, $\mathbf{q}^{(e)}$is the nodal displacement vector, $\mathbf{f}^{i(e)}$ represents the internal forces and momentum, $\mathbf{f}^{c(e)}$ the external forces and momentum and $\mathbf{f}^{c(e)}$ element distributed loading.

3. RESULTS

In this section, a test structure, described in the literature, was used to evaluate the integration method adopted. This structure consists of a cantilever beam, as illustrated in Fig. 2a. This beam model was firstly implemented by Cao et al. (2005). The structure dimensions are: 0.3 m of length, 0.01 m of cross section width and 0.005 m of thickness. The values adopted for Young modulus and density are 2.08×10^8 Pa e 3.0×10^3 kg/m³, respectively.

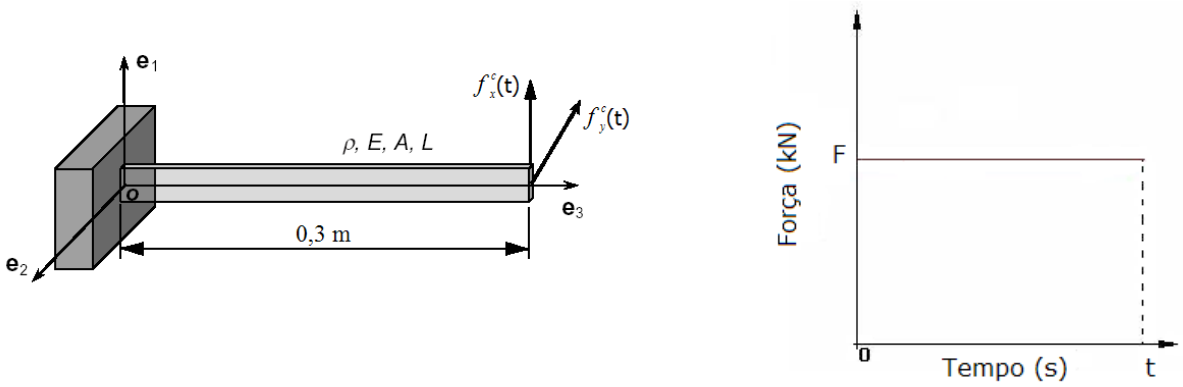

(a) (b)

Figure 2 – Simulated model: (a) test structure; (b) time varying force applied at the free end of the test structure

It is important to emphasize that the same test structure was initially used by the authors in order to validate the implemented algorithm of the Cosserat beam theory for dynamic analyses. The omission of these results is justified in order to keep focus in the integration methods used to solve the nonlinear equations, which are the basis of the methodology. As presented in Borges et al. (2009) and Borges (2010), an essential aspect when dealing with nonlinear systems is the performance of the methods used to integrate the equations of motion, especially accuracy and stability.

Therefore, the realization of the numerical simulations presented in this work has demanded significant efforts in order to identify the most suitable techniques to be employed in association with the Cosserat theory.

Another aspect also investigated in this section was the influence of the order of approximations of the shape functions on the accuracy of the responses obtained by integration.

The integration methods evaluated in the simulation cases were: the Composite Implicit Time Integration Scheme, proposed by Bathe (2007), and referenced here as *Newmark conservative*; the Newmark method combined with the Newton-Raphson algorithm, proposed by Géradin and Rixen (2001); and the method of Runge-Kutta of fourth order with variable time step, available in the commercial software Matlab.

Several simulations were performed using approximations of order two and three, and for each case, the amplitude of the force was gradually increased and the respective time response was calculated using the three integration methods studied. In the first test, the structure was modeled using approximations of order two and subjected to a force of 0.001N applied in *x* direction in the form of a step function localized at the free end of the beam. Several simulations were conducted, but the only algorithm that has converged was that one based on Newmark conservative method. On the other hand, when approximations of order three were employed, all three integration methods converged. In all cases investigated, the structure was discretized in 10 elements of equal lengths. Fig. 3 shows the time response history corresponding to the displacement at the free end of the test structure along the *x* direction.

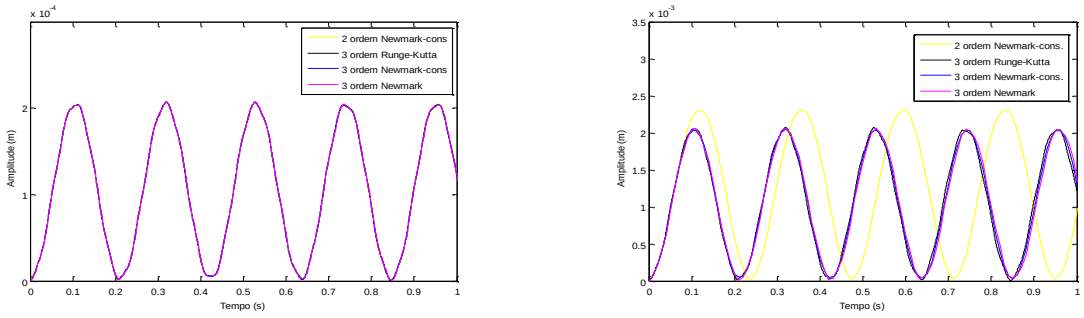

(a) (b)

Figure 3 – Comparison between the different approximations for the shape functions and integration methods for different loading cases: (a) F=0,001 N;(b) F=0,01 N.

In Fig. 3a, one can observe that both shape functions approximations and all integration methods have converged to the same result. However, it was necessary to use different time steps for each method. This fact has occurred because the resolution of the nonlinear equations is performed at each time step, and a residue is minimized until a predefined value, defined by the analyst. Therefore, the method diverges when it is not capable of satisfying this criterion. In the simulation cases studied, whenever the algorithm diverged, another simulation was initiated with a time step of one half of the previous one and the convergence was tested again

Comparing the results obtained using two different orders of approximation for the shape functions, it is possible to observe different sizes of time step for the same integration method. In the case where the Newmark conservative method was employed, the time discretization was $1.0x10^{-4}$ s for the approximations of order two and $1.0x10^{-2}$ s for the approximations of order three. For all other methods, only the approximations of order three have converged, and the time steps used were: $1.0x10^{-2}$ s for Newmark and values varying from $1.058x10^{-8}$ s to $1.10x10^{-5}$ s, and mean value of $5.88x10^{-6}$ for Runge-Kutta method. At this point, it is important to emphasize that the time step is a decisive parameter, influencing directly the computational effort required for the simulations.

The results obtained when the force applied was increased to 0.01 N are presented in Fig. 3(b). In this case, it is possible to observe the differences between the results obtained from approximations of order two and three, considering the same integration method. These differences are remarkable in the amplitudes, in the response period, and the time step used are also different. In the approximations of order three, the time step was the same used for the previous simulation case, in other hand, for the approximations of order two the time step had to be reduced to $1.0\ x10^{-5}$ s in order to achieve convergence, requiring a higher time of processing.

The integration methods based on approximations of order three have converged to the same results. The time step used for Newmark method was $1.0x10^{-2}$ s, and for the Runge-Kutta method the time step varying from $1.38\ 0x10^{-5}$ s to $1.08x10^{-5}$ s, and mean value of $5.70x10^{-6}$ s.

Comparing Figs. 3(a) and 3(b), one can notice that the displacement amplitudes (except the responses calculated based on approximations of order two) are proportional to the value of the applied force. This fact confirms the linearity of the test structure behavior, justified by the small magnitude of forces and displacements involved.

An important observation concerns to the discretization by finite element method using approximations of order two, which was insufficient in terms of precision. It was also noted that, for F=0.1 N the methodology based on those approximations, and using the conservative Newmark integration method , the numerical convergence could not be achieved, even reducing drastically the time step used. This fact leads to the option of employing the formulation based on the approximations of order three. Therefore, in the simulation cases that follow, the force applied was progressively increased, assuming amplitudes of 0.1 N, 1.0 N, 10.0 N, and 100 N in order to evaluate the integration algorithms for the approximations or order three for the shape functions from Cosserat beam theory. The obtained responses from the applied force of 0.1 N are presented in Fig. 4(a).

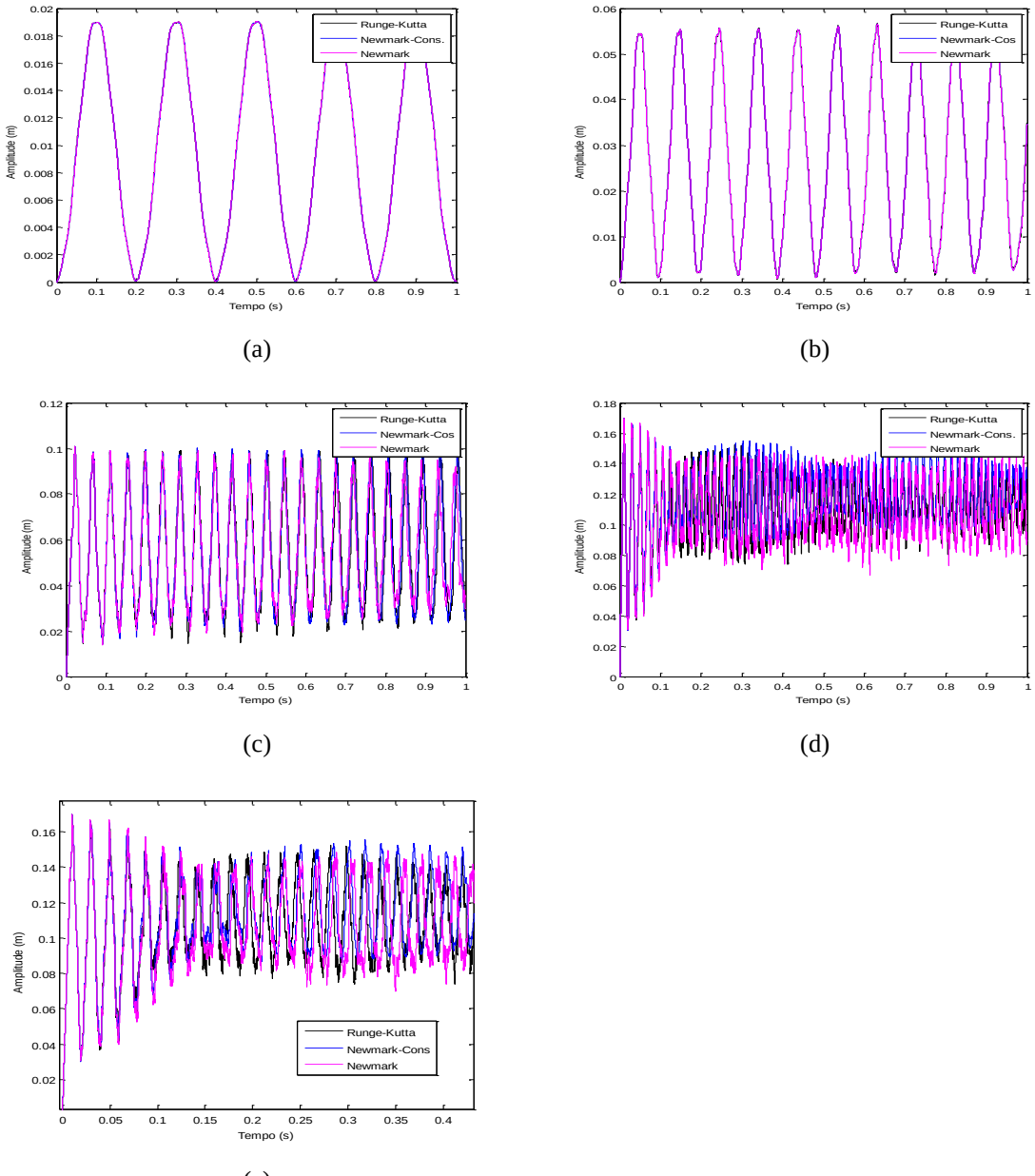

Figure 4 – Comparison between the responses obtained from different integration method for: (a) F=0.1 N; (b) F=1.0 N; (c) F=10.0 N; (d) F=100.0 N and (e) Details of item (d).

The time step used for Runge-Kutta method was varied from 1.38×10^{-9} s to 1.10×10^{-5} s, and mean value of 5.68×10^{-6} s. For Newmark conservative method the time step used was 1.00×10^{-3} s, and for Newmark the time step was 2.00×10^{-4} s

In Fig. 4(b) the time responses for F=1.0 N are presented. In this case, the time discretization used for Runge-Kutta method was varying from 1.38×10^{-10} s to 1.03×10^{-5} s and mean value of 5.5×10^{-6} s. For Newmark conservative method the time step used was 1.0×10^{-3} s and for Newmark the time step was 2.0×10^{-4} s.

Fig. 4(c) shows the time responses calculated for F=10 N. The time discretization for Runge-Kutta method varied between $1.38x10^{-11}$ s and $5.5x10^{-6}$ s, and mean step of $5.23x10^{-6}$ s.The Newmark conservative and the Newmark methods have presented the same time step of $1.0x10^{-4}$ s. Observing Figure 4(c), it can be seen that the results of Newmark method are in disagreement with those provided by the other two integration methods. It is important to emphasize that, considering the previous simulated cases, the frequency components presented now are higher, and the amplitudes are no more proportional to the applied force, revealing deviations from linear behavior.

At last, the time response obtained for F=100.0 N is presented in Fig. 4(d). In this case, the time step used in the Runge-Kutta method was varying from $1.38x10^{-12}$ s a $7.56x10^{-6}$ s and mean step of $4.44x10^{-6}$ s. The conservative Newmark method has achieved convergence using a time step of $5.00\ x10^{-5}$ s, while the integration method of Newmark converged with a time step of $2.0\ x10^{-5}$ s. Observing Figs.4(c)-(e), it is possible to verify that the responses present a wider frequency content, and the amplitudes begin to suffer variations along the time, which can be attributed to the influence of nonlinear effects.

After the investigation of the approximations o second and third order, and three different integration methods, it is possible to draw some considerations about the computational time spent with simulations imposing large displacements. The integration methods of Newmark conservative and Newmark took about 1.5 hours to achieve convergence. On the other hand, the integration method of Runge-Kutta took about seven days of processing, which can be attributed to the small time step necessary to achieve convergence.

In order to explain the significant difference observed in the period response calculated for the free end of the structure, as illustrated in Fig. 4 (a)-(d), it is important to consider that, in opposition to the linear beam formulation (Euler-Bernoulli), the Cosserat beam theory takes into account the effect of stiffening due to the axial components of the force applied to the free end of the beam. Such a component will be more pronounced as the displacement in the *x* direction becomes larger. This phenomenon appears due to the coupling between the longitudinal and transversal effects that increase the oscillation frequency as predicted by Cosserat beam theory. This effect is known in literature as stress stiffening (Bokaian, (1988); Bokaian, (1990)).

4. CONCLUSIONS

Considering to the methodology of structural modeling based on Cosserat beam theory, which leads to nonlinear equations of motion, a particular effort was undertaken in tests of several numeric integration algorithms. These tests were performed to choose the best adapted algorithms to perform step by step integration in the time domain. In these simulations, the Newmark conservative method was noticed to be more stable and accurate in the numeric integration and, therefore, it was chosen to be used in the future works.

Another investigated aspect concerns the approximation order of the shape form functions used for the discretization equations by the finite elements technique. In this case, were examined the second and third order approximations. It was observed that, with the use of a same integration method, the second order approximations do not allow to obtain numeric convergence, even by decreasing the time step. On the other hand, with the third order approximations the convergence was reached without difficulties. It should be noticed that there are few works in the literature that use approaches of the third order. This can be explained by the high complexity of the resulting equations, which result from a large volume of algebraic manipulations that could be not accomplished without the computational program resources of symbolic manipulation.

Numerical simulations showed the capacity of the Cosserat beam theory for the modeling of the vibratory behavior in nonlinear regime, which is characterized when the amplitude of displacements and rotations are larger and not proportional the applied force. It was also observed that the increase of the oscillation frequency due to the stress stiffening caused by the axial force component, can be accounted for by the modeling methodology.

5. ACKNOWLEDGEMENTS

The authors gratefully acknowledge the Brazilian Research Council – CNPq and Parana State Research Agency Araucaria for the continued support to their research work and funding through grants and scholarships.

6. REFERENCE

ALAMO, F. J. C. Dinâmica de estruturas unidimensionais esbeltas utilizando o contínuo de Cosserat. 2006. 124p. Tese de doutorado-Departamento de Engenharia Mecânica, Pontifícia Universidade Católica do Rio de Janeiro, Rio de Janeiro.

ANTMAN S. S. Nonlinear Problems of Elasticity, Applied Mathematical Sciences. 2.ed. New York: Springer-Verlag, 1995. 884p.

ARFKEN, G.; WEBER, H. J.; HARRIS, F. Mathematical Methods for Physicists. 5.ed. Academic Press Inc., San Fiego. 2000. 1112p.

BATHE, K. J. Conserving Energy And Momentum In Nonlinear Dynamics: A Simple Implicit Time Integration Scheme. Computers and Structures. v.85, p. 437–445. 2007.

BOKAIAN, A. Natural frequencies of beams under compressive loads. Journal of Sound and Vibration. v. 126, p. 49–65. 1988.

BOKAIAN, A. Natural frequencies of beams under tensile loads. Journal of Sound and Vibration. v. 142, p. 481–498. 1990.

BORGES, A. S. Desenvolvimento de procedimentos de modelagem de interação fluido- estrutura combinando a teoria de vigas de Cosserat e a metodologia de fronteira imersa. 2010. 199 f. Tese de Doutorado, Universidade Federal de Uberlândia, Uberlândia, MG.

BORGES, A. S.; LUZIANO, W. P. ; RADE, D. A.; SILVEIRA NETO, A., A Numerical Study of Cosserat Beam Theory Applied to the Modeling of Subsea Risers. In: 20th International Congress of Mechanical Engineering, 2009, Gramado-RS. Proceedings of COBEM 2009.

CAO, D. Q.; DONGSHENG, L.; CHARLES, H.; WANG, T. Nonlinear dynamic modelling for MEMS components via the Cosserat rod element approach. J. Micromech. Microeng. v. 15, p. 1334–1343. 2005.

CAO, D. Q.; DONGSHENG, L.; CHARLES, H.; WANG, T. Three Dimensional Nonlinear Dynamics of Slender Structures: Cosserat Rod Element Approach. International Journal of Solids and Structures. v. 43, p. 760-783. 2006.

GÉRADIN, M.; RIXEN, D. **Theory and application to structural dynamics**. 2.ed.John Wiley & Sons. 2001.

PESCE, C. P. Mecânica de cabos e tubos submersos lançados em catenária: uma abordagem analítica e experimental. Journal of Fluid Mechanics v. 116, p.77-90. 1997.

SANTOS, C.M.P.M. Análise de Estruturas Esbeltas Offshore Sujeitas à Vibrações Induzidas por Vórtices (VIV). 2005. Tese de Doutorado, Programa de Engenharia Civil, COPPE/UFRJ, Rio de Janeiro, Brasil.

SIMO, J. C. A finite strain beam formulation – the three-dimensional dynamic problem part I. Computer Methods in Applied Mechanics and Engineering. v.49, p. 55-70. 1985.

VU-QUOC L.; SIMO, J. C. A Three-Dimensional Finite Strain Rod Model Part II: Computational Aspects. Computer Methods in Applied Mechanics and Engineering. v. 58, p. 79-116. 1986.

7. RESPONSIBILITY NOTICE

The following text, properly adapted to the number of authors, must be included in the last section of the paper:
The author(s) is (are) the only responsible for the printed material included in this paper.